Analyst

PAPER

View Article Online
View Journal

Cite this: DOI: 10.1039/d6an00237d

Impact of preparation methods and storage conditions for optimization of the fecal metabolome storage stability

Vladyslav Dovhalyuk and Daniel Globisch *

Untargeted fecal metabolomics has gained a higher scientific interest in the past decade, due to the increased importance of the gut microbiome metabolism. It is highly sensitive to preanalytical variations. However, the impact of sample collection, storage, and preparation on the metabolome composition remains insufficiently studied. In this study, we have systematically evaluated the effects of two sample preparation protocols: 5% DMSO/water solvation, followed by solvent substitution to methanol, referred to as the double-liquid extraction (DLE) protocol in this study, and methanol homogenization with FastPrep lysing matrices. Additionally, we examined long-term storage at −80 °C in a freezer, including fresh and freeze-dried samples, with and without methanol, at various stages of sample preparation. Global feature coverage and sensitivity analyses revealed that efficient mechanical homogenization is critical for maximizing metabolite recovery, particularly for intracellular and microbially derived compounds (enterolactone, allolithocholic acid). However, complete depletion of water and extraction in pure methanol resulted in a reduced feature coverage and lower signal intensities, particularly for polar metabolites such as proline and tyrosine. In the case of a freeze-drying step, reintroduction of water during sample preparation substantially improved extraction efficiency, underscoring the importance of maintaining controlled hydration of the fecal matrix to improve the solubility of the metabolite mixture.

Received 3rd March 2026,
Accepted 3rd June 2026

DOI: 10.1039/d6an00237d

rsc.li/analyst

Introduction

Fecal samples represent one of the most complex and information rich biological matrices that has found more attention in human health research.[1] The fecal metabolome contains many endogenous and dietary metabolites including xenobiotics, microbial products, and host-microbiome co-metabolites, providing an important window into gastrointestinal metabolism and microbial activity.[2] The human gut microbiome plays an important role in digestion, immune regulation, inflammation, and metabolic homeostasis. Disruption of this ecosystem has been linked to a wide range of diseases, including inflammatory bowel disease, colorectal cancer, metabolic disorders, neurological conditions, and pancreatic diseases.[3] As a result, fecal samples have become a resource that has gained an increasing importance for clinical diagnostics, epidemiological cohorts, and nutritional interventions.

Upon the initial breakthrough findings of the metagenomics analyses, fecal metabolomics has now emerged as a powerful tool to profile microbial metabolism to improve the understanding of the chemical interplay between the gut microbiota and their host.[4] However, the collection and handling of fecal samples remain major challenges in fecal metabolomics. The fecal material undergoes biochemical changes immediately after defecation due to ongoing microbial activity, enzymatic reactions, exposure to oxygen, and temperature fluctuations. In established routine clinical workflows, delays between sample collection and laboratory processing are often unavoidable as it has been investigated in several studies.[5,6] Transport conditions, patient compliance, and temperature differences during transit can substantially influence the sample composition.[7] As a result, standardizing fecal sample handling from collection to laboratory analysis is critical for ensuring reproducible and biologically meaningful results.[8]

Storage conditions add another layer of complexity. Fecal samples can be stored freshly frozen, lyophilized, or preserved in stabilization solutions with organic solvents such as methanol. Each strategy can differentially affect microbial viability, enzymatic activity, metabolite stability, and the formation of new compounds through degradation of labile compounds.[9–11] Despite widespread use of these approaches, there is currently no clear consensus on which preparation and storage conditions best preserve the original fecal metabolome.[1,12,13]

In metabolomics studies, sample preparation introduces additional variability. Unlike plasma, urine, or tissue, fecal material lacks a standardized extraction strategy because of its

Department of Chemistry for Life Science, Science for Life Laboratory, Uppsala University, Sweden. E-mail: Daniel.globisch@kemi.uu.se

heterogeneous composition, variable water content, and high microbial load. Moreover, the optimal workflow for metagenomic microbiome profiling is not suitable for standard global metabolomics analysis. Methods developed for microbial DNA stabilization do not guarantee chemical stability of metabolites and chemicals used for DNA/RNA preservation are not compatible for mass spectrometric analysis. In here, we systematically evaluate combinations of sample preparation and storage conditions to assess their relative impact on the fecal metabolome profiles under a controlled experimental setting to provide a comparative analytical framework for understanding workflow-dependent variability.

Experimental

Materials and methods

Sample collection and study design. Stool samples were collected from a healthy adult volunteer for untargeted metabolomics profiling. Sampling was performed on seven days within a 10 day period. For each collection, the freshly obtained stool was homogenized manually, and approximately 60 mg were distributed into 33 aliquots, corresponding to 11 sample preparation and storage conditions in triplicate (Table 1). All aliquots were processed according to their assigned condition within 1 hour of collection to minimize metabolite degradation or microbial transformation. In the next step, the samples were placed into the −80 freezer for long-term storage, which was 5–6 months depending on the condition of the pre-storage protocol and the sampling day. After long-term storage, all samples were processed according to their respective post-storage protocols and analyzed in a single LC-MS sequence.

Prior to the collection of the samples, each aliquot tube was loaded with a mixture of isotopically labeled stability standards to monitor extraction reproducibility and signal stability throughout the study. Tubes were spiked with isotopically labeled tyrosine ($^{13}C_9$, ^{15}N, 5 μg mL^{-1}), phenylalanine ($^{13}C_9$, ^{15}N, 10 μg mL^{-1}), and valine ($^{13}C_5$, 30 μg mL^{-1}), followed by drying using a SpeedVac.

Each daily stool sample was divided into 11 conditions designed to evaluate the impact of the extraction method, hydration state, and storage solvent on metabolome stability. Conditions were selected based on commonly used protocols in metabolomics workflows: for "fresh storage" conditions, aliquots were processed immediately without freeze-drying. "Dry storage" conditions involved overnight lyophilization. Homogenization with lysis matrix D, lysis matrix E, and double-liquid extraction corresponded to variations in mechanical disruption and solvent ratios, as detailed below. Methanol storage conditions consisted of immediate submersion of the aliquot in cold LC-MS grade methanol (100%) to rapidly inactivate enzymatic and microbial activity. Milli-Q water and MS grade solvents were used throughout the experiment. All mixture proportions are expressed as v/v.

Two validated extraction protocols were used, depending on the condition type:

1. Double-liquid extraction protocol

Samples after freeze-drying overnight, weighed and solvated with dimethyl sulfoxide (DMSO) and water (1 : 20) to a final equivalent of 60 mg mL^{-1}. Tubes were sonicated for 5 min and centrifuged (13 400*g*, 5 min). Supernatants were normalized by volume across all samples, aliquoted, and freeze-dried overnight. For the second extraction, dried pellets were reconstituted in 50 μL water, followed by the addition of 240 μL cold methanol. After a brief freezing step (−20 °C, 1 h), samples were centrifuged, supernatants collected, dried with SpeedVac, and reconstituted in 50 μL 5% acetonitrile (ACN)/water prior to LC-MS injection.

Condition 1 aliquots were frozen within 30 min after collection, and sample preparation was performed after long-term storage. Condition 3 aliquots were freeze-dried overnight, and the dry pellets were stored at −80 °C, and sample preparation was continued after long-term storage. Condition 11 aliquots were completely prepared before long-term storage, and the dry pellets before reconstitution in 5% ACN were frozen.

2. Homogenization with lysing matrices D and E (FastPrep-based protocols)

Selected conditions employed bead-beating homogenization adapted from the solid tissue extraction protocol. Aliquots were mixed with 4 μL of 100% methanol per mg of fresh fecal material. For lysing matrix D, homogenization beads were added in a 1 : 1 mass ratio to the Eppendorf tubes. For lysing matrix E, commercially available Fast-Prep tubes

Table 1 Studied sample preparation and storage conditions

No.	Sample preparation	Freeze-dried after collection	Long-term storage condition	Collection days
1	Double-liquid extraction	No	Fresh storage	1–7
2	Homogenization (lysing matrix D)	No	Fresh storage	1–7
3	Double-liquid extraction	Yes	Dry storage	1–7
4	Homogenization (lysing matrix D)	Yes	Dry storage	1–7
5	Homogenization (lysing matrix D)	No	Methanol storage	1–7
6	Homogenization (lysing matrix D)	No	Homogenized storage	2–3, 5–7
7	Homogenization (lysing matrix D)	Yes	Methanol storage	1–7
8	Homogenization (lysing matrix D)	Yes	Homogenized storage	1–7
9	Homogenization (lysing matrix E)	No	Homogenized storage	2–5
10	Homogenization (lysing matrix D)	No	Fully prepared and dried	2–7
11	Double-liquid extraction	Yes	Fully prepared and dried	1–7

that already contained beads were used. Both lysing matrices were obtained from MP Biomedicals. Samples were homogenized using FastPrep at 4 m s^{-1} in three cycles (20 s shaking, 30 s rest). Supernatant were aliquoted to new tubes, incubated at −20 °C for 1 h, centrifuged, and dried by SpeedVac. Final reconstitution was performed in 5% ACN/water at a volume normalized to sample weight.

Conditions 2, 5, 6, 9, and 10 were treated as fresh samples. Conditions 4, 7, and 8 were freeze-dried before homogenization. Conditions 2 and 4 were frozen fresh and freeze-dried, respectively, and sample preparation was performed after long-term storage. Conditions 5 and 7 were solvated with Methanol and placed for long-term storage, with sample preparation followed before analysis. Conditions 6, 8, and 9 were homogenized with respective beads and frozen with beads in tubes. Condition 10 was completely prepared before storage and frozen as a dry pellet before final reconstitution.

Storage strategies differed by hydration state (fresh *vs.* dried) and solvent environment: fresh samples were kept on ice before homogenization and extraction or long-term storage at −80 °C. Dried samples underwent lyophilization and were stored dry at −80 °C before starting additional steps. Methanol-stored samples were immediately submerged in ice-cold MS-grade methanol to suppress metabolism. Non-methanol storage conditions kept the fecal material in its assigned state (fresh or dry) at −80 °C until extraction. All samples were protected from thawing, oxygen exposure, and microbial activity as much as possible. No sample underwent more than one freeze–thaw cycle. Samples were in long-term storage for at least 5 months.

Due to practical constraints during the sample preparation and storage, not all condition-day combinations were available for all sampling days (Table 1). In particular, conditions 6 and 10 were originally planned across all sampling days, but selected condition-day combinations were excluded due to incomplete replicate sets as a result from sample loss. To maintain consistency in the replicate structure, only condition-day combinations with complete triplicates were included for statistical analysis. Condition 9 (lysing matrix E) was additionally included as an exploratory condition with limited combinations and was therefore excluded from the multifactorial analysis.

LC-MS analysis. The UHPLC-MS/MS analysis was performed in a Maxis II ETD Q-TOF mass spectrometer (Bruker Daltonics, Germany) using an electrospray ionization (ESI) source with an Elute UHPLC system (Bruker Daltonics, Germany). The separation was performed on an Acquity UPLC HSS T3 column (1.8 μm, 100 × 2.1 mm) from Waters Corporation. Milli-Q water with 0.1% formic acid was used as mobile phase A, and MS-grade methanol with 0.1% formic acid was used as mobile phase B. The column temperature was kept at 40 °C, and the autosampler temperature was kept at 5 °C. The flow rate was set to 0.2 mL min^{-1} with an injection volume of 5 μL. The gradient used was as follows: 0–2 min, 0% B; 2–15 min, 0–100% B; 15–16 min, 100% B; 16–17 min, 100–0% B; 17–21 min, 0% B. The system was controlled using the Compass HyStar software package from Bruker (Bruker Daltonics, Germany). High-resolution mass spectra were acquired in positive and negative mode at a mass range of m/z 50–1200. Data acquisition was performed in AutoMSMS mode (data-dependent acquisition, DDA) with a cycle time of 0.5 s and a ramped collision energy from 20 to 50 eV. A solution of sodium formate [10 mM in a mixture of 2-propanol/water (1 : 1)] was used for internal calibration at the beginning of each run, in a segment between 0.1 and 0.3 min. The samples were injected into the UPLC-MS system in a randomized order with QC samples injected at the beginning and end of the sample list in both ionization modes, as well as after every eight samples. The standard deviation of the mass calibration for all injections was below 0.5 ppm.

Data preprocessing and statistical analysis. The MZML converted instrumental files were processed using the XCMS R package (version 4.2.1) for peak peaking and retention time correction, in both positive and negative ionization modes.[14,15] After XCMS, Systematic Error Removal using Random Forest (SERRF) normalization was performed using an R script (Shiny-SERRF from UC Davis).[16] Features with QC intensities> 20 000 ion count for positive ion mode and intensities > 10 000 ion count for negative ion mode, retention time >1 min and <18 min, and RSD of the QCs < 30% were selected for further statistical analysis. The intensities of the internal standards and the QC samples were plotted against the UPLC-MS/MS sample injection order to evaluate the stability and performance of the experimental set over time. An overview of the data was provided by principal component analysis (PCA).

Statistical analysis for each metadata factor was performed using a linear regression model with cofactor adjustment utilizing in-house R scripts. For each feature, models of the form intensity ~ factor_of_interest + sampling_day + cofactors were fitted, where one factor was evaluated at a time while adjusting for the remaining experimental variables. Linear models were fitted using the available observations without imputation of missing condition-day combinations. Sampling day was included as a covariate to account for temporal variability. For Fold change analysis, estimated marginal means (EMM) were calculated using emmeans R package.[17] *P*-Values were not adjusted for multiple testing, and statistical significance was interpreted in combination with effect size thresholds and feature filtering criteria, consistent with the exploratory and method development nature of the study.

For untargeted selectivity and sensitivity analysis, stable features were filtered based on the following criteria: average intensity greater than 20 000 ion counts and a relative standard deviation (RSD) below 30% within a given sampling day and experimental condition. Selectivity was defined as the breadth of metabolite detection and quantified as the number of stable features per condition and sampling day. Sensitivity was defined as the typical signal intensity of detectable metabolites within a given condition. Sensitivity was quantified by calculating, for each sampling day and condition, the median of the average intensities of all stable features passing the filtering criteria. We used the ggplot2 R package for creating statistical plots, and Biorender for graphical illustrations.

Compound identification. Significant features and molecules of interest were primarily annotated by HMDB database (https://www.hmdb.ca) based on *m*/*z* value, high resolution mass and AutoMSMS fragmentation spectra.[18] The SIRIUS platform was used for spectra screening.[19–21] The CANOPUS tool was utilized as part of the SIRIUS software to predict compound classes of molecular features.[22] An in-house MS/MS screening R script utilizing MetaboAnnotation and CompoundDb packages was used.[21] The standards were acquired under the same conditions as the sample acquisition method. Meanwhile, MassBank (release 2021-03) was also used to screen the MS/MS.[23]

We have used a combination of structure elucidation with our in-house chemical library of authentic standards as well as the SIRIUS software to classify metabolites into four confidence levels (CL).[24]

Ethics declaration. Fecal samples were obtained from a healthy individual with informed consent. An ethical review statement was not necessary according to the Swedish Ethical Review Act (lag (2003:460) om etikprövning av forskning som avser människor), as samples were given voluntarily, fecal sampling is non-invasive, non-traceable to the individual, and no personal information was used.

Results and discussion

Due to the high diversity of workflows applied across fecal metabolomics studies, we designed a study to evaluate different aspects of sample preparations and storage conditions for this biochemically unstable sample type. The double-liquid extraction protocol is based on initial freeze-drying of the fecal material, followed by water solubilization with a small amount of DMSO, and sequential solvent replacement with methanol for the metabolite extraction and protein precipitation. This procedure has been routinely applied as it has demonstrated a robust and reproducible performance across fecal metabolomics studies.[25–28] On the other hand, methanol-based collection, storage, and extraction workflows are rapidly gaining popularity in the fecal metabolomics community, including commercially available homogenization lysing matrices and the increasing adoption of methanol quenching, both at the collection time and during storage.[7,29,30] While the fecal collection processes and sample preparation have been extensively evaluated, the long-term storage practices remain understudied. The gold standard is considered snap freezing of a fresh material and storage at −80 °C until the sample preparation and analysis in clinical settings.[31–33] However, this approach is not directly compatible with methanol-based collection workflows, where samples must remain in methanol during the storage. Lyophilization *via* freeze-drying prior to storage represents another suitable option for long-term preservation. Although lyophilization is typically integrated into extraction workflows rather than performed immediately upon collection, dried samples are generally more chemically stable and less susceptible to microbial degradation due to the absence of water.[30] Implementing freeze-drying at the point of collection may be challenging outside laboratory settings including in hospitals and during collection at home. However, as samples are in many cases expected to undergo prolonged storage before their analysis, we have tested whether pre-storage freeze-drying may provide substantial benefits for metabolite stability. Our study incorporates both fresh frozen and freeze-dried states to compare their respective impacts for long-term storage of fecal material (Fig. 1).

Fecal samples were separately prepared based on the 11 conditions of different sample preparation protocols and storage (Table 1) and subsequently investigated each condition *via* UHPLC-MS/MS analysis in a randomized sequence with quality control samples included. The mass spectrometric data were pre-processed using XCMS, that was followed by statistical analysis *via* in-house R scripts.

The global feature coverage and sensitivity analysis offers a complementary, systems level perspective on the performance of the different methodologies. Summarizing 15 658 of untargeted features across all conditions and sampling days provides the possibility to obtain an integrated evaluation of extraction robustness, analytical sensitivity, and temporal variability that cannot be captured by isolated factor-based analyses alone.

Across conditions, global feature coverage revealed consistent differences in the number of stable, detectable features recovered by each protocol ranging from 1000–5000 (Fig. 2A), whereas sensitivity heatmaps further discriminated conditions based on the overall signal intensity of stable metabolites (Fig. 2B). Together, these complementary metrices provide a balanced evaluation of the analytical performance, capturing both the breadth of metabolite recovery (selectivity) and the typical signal strength of extracted features (sensitivity; Fig. 2C). Protocols combining beads-based homogenization with non-lyophilized samples generally achieved higher feature coverage and greater signal intensities, indicating more efficient extraction of a broader range of metabolites. In contrast, freeze-dried samples reconstituted in pure methanol consistently yielded fewer detectable features and reduced signal intensities. Although the DLE protocol showed intermediate performance in terms of global selectivity and sensitivity, it demonstrated comparatively high robustness toward variations in sample preparation and storage conditions. Importantly, differences observed at the level of global selectivity and sensitivity were modest when compared with the pronounced day-to-day variability present in the dataset, likely reflecting biological and pre-analytical factors such as dietary intake and sampling time. However, despite this dominant temporal variability, several metabolite classes exhibited clear and reproducible preferences for specific storage and extraction strategies. These findings underscore the necessity of strictly standardized sample preparation and storage protocols within and across studies to minimize technical variability and to avoid confounding intra- and inter-individual biological differences.

Multivariate principal component analysis (PCA) revealed a clear clustering mainly based on the extraction and homogenization approach (Fig. 3A). Samples prepared using a double-

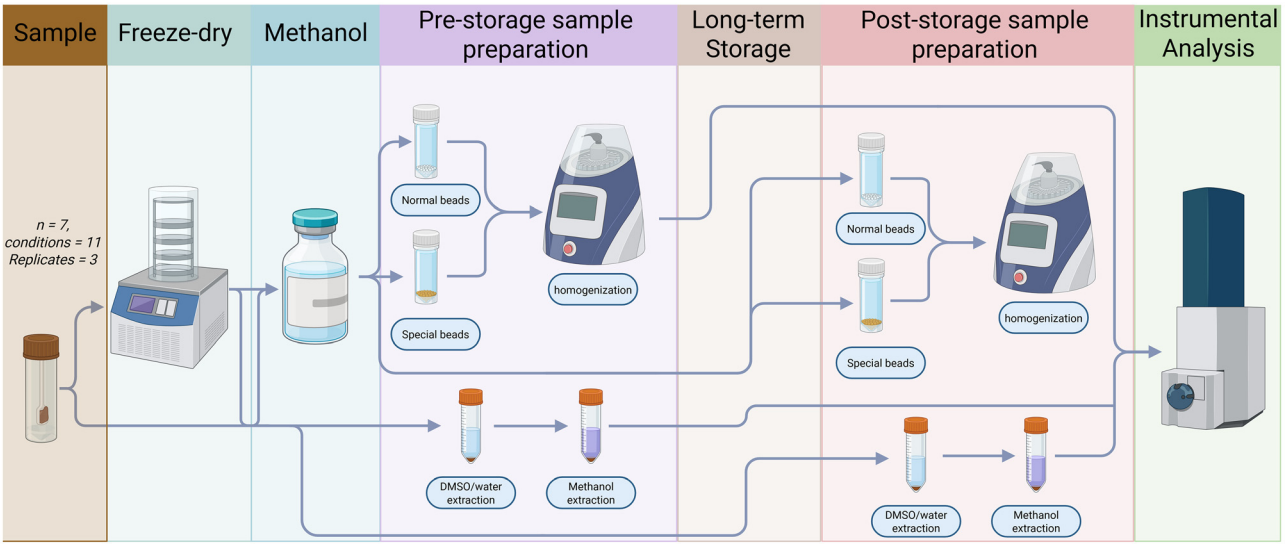

Fig. 1 Overview of the study design. Fecal samples were collected on 7 different days and split into 11 sample preparation/storage conditions (7 samples, 33 aliquots, 11 conditions, 3 replicates). Conditions were composed of a unique combination of study factors, such as freeze-drying upon collection, addition of methanol before long-term storage (5 months), sample preparation protocols (double-liquid extraction, homogenization with 2 different lysing matrices D and E), and different stages of sample preparation before storage. Sample preparation was completed upon thawing, and global metabolomics analysis was performed using UHPLC-MS/MS following standardized sample preparation and quality control.

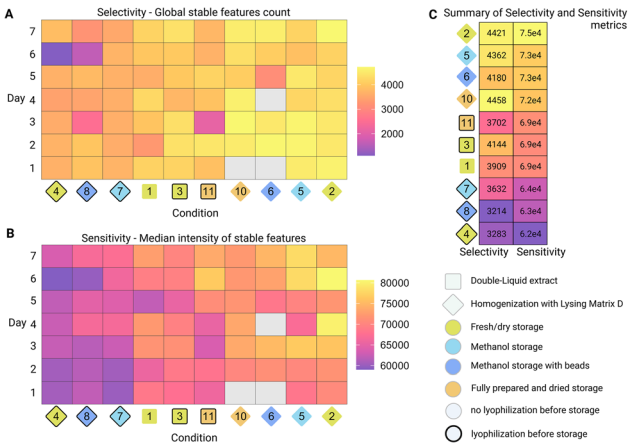

Fig. 2 Global untargeted feature-based coverage and sensitivity heatmaps across tested conditions. (A) Global feature coverage. For each condition and sampling day, features were counted if they met stability criteria based on triplicate measurements (mean intensity > 20 000 ion counts; RSD < 30%). Presented as feature count. (B) Sensitivity based on global coverage features. Using the stable feature set defined in panel A, sensitivity was quantified for each condition and day as the median of mean triplicate intensities of all stable features. Presented as feature intensity ion count. (C) Summary of previous two metrics. Presented as a mean of all days. All plots *y*-axis ordered based on all days mean of median intensities of stable features.

liquid extraction protocol (5% DMSO/water solubilization followed by methanol extraction) formed a distinct cluster, indicating a characteristic metabolite pattern associated with the solvent-based extraction.

In contrast, beads-based homogenization protocols using lysing matrix D from MP Biomedicals have a much wider spread, while lysing matrix E clustered more closely. Lysing matrix E contains additionally smaller spheres to also homogenize microbial cells completely. Noteworthy is the fact that only four instead of seven samples were treated with matrix E. Matrix E conditions were not included in the multifactorial analysis due to the smaller sample size and the lack of combinations with other factors. Thus, matrix D and E were compared separately (Fig. S1). These differences likely stem from an improved mechanical disruption efficiency, bead composition, and physicochemical selectivity of each workflow. QC samples consistently formed a tight cluster across all analyses, confirming the high analytical reproducibility and validating that the observed variations are originated from biological and methodological factors.

Daily sampling over 10 days from one healthy volunteer enabled assessment of short-term biological variability within a single individual. The PCA plot of sampling days demonstrates the close clustering of the first five days, while quite pronounced day-specific clustering was observed for days 6 and 7 (Fig. 3B). This observation is consistent with previous reports that the individual fecal metabolome varies substantially over time due to changes in diet, microbial activity, and intestinal transit.[34] Despite these differences, most days partially overlapped and only gradually shifted, reflecting the shared individual core metabolome. These observations highlight the intra-individual temporal variability, which is important when designing longitudinal fecal metabolomics studies and reinforces the necessity of multi-day sampling when feasible.

To closely investigate the differences between sample preparation protocols, we compared the DLE workflow with a procedure using bead-based homogenization using lysing matrix

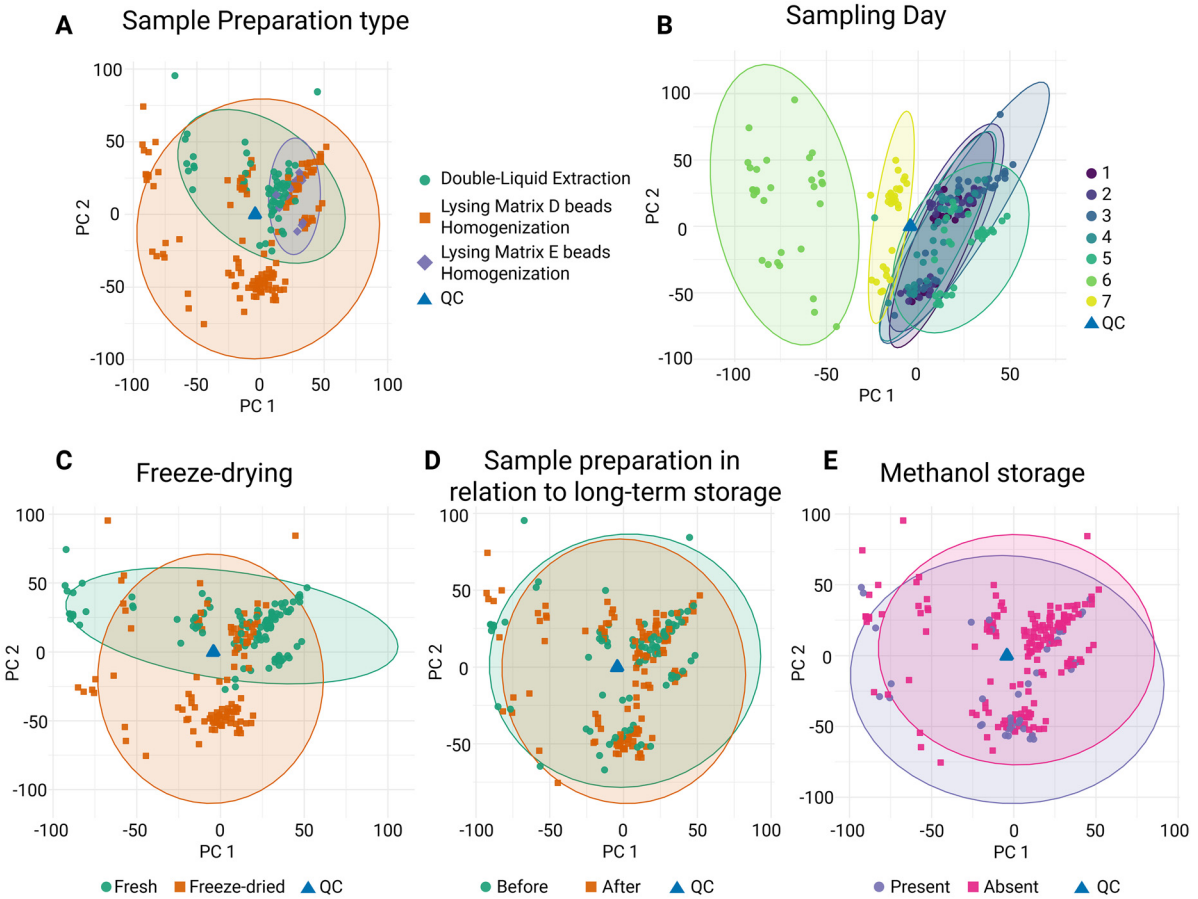

Fig. 3 Multivariate analysis of sample collection, preparation, and storage factors. (A) PCA plot of the sample preparation protocol. Green circles: double-liquid extraction protocol utilizing DMSO/water extraction followed by methanol extraction. Orange rectangles: lysing matrix D bead-based homogenization. Purple diamonds: lysing matrix E bead-based homogenization. Blue triangles: QC samples. (B) PCA plot showing the effect of sampling day across seven independent stool collections. (C) PCA plot comparing fresh *versus* freeze-dried sample handling. Green circles: fresh samples and orange rectangles: freeze-dried samples. Blue triangles: QC samples. (D) PCA plot illustrating sample preparation timing in relation to long-term storage. Green circles: samples prepared before long-term storage, and orange rectangles: after long-term storage. Blue triangles: QC samples. (E) PCA plot assessing the influence of long-term storage in methanol. Purple circles: samples where methanol was present during storage, and pink rectangles: those stored without methanol. Blue triangles: QC samples.

D. For this comparison, we applied a linear regression model adjusted for the sampling day, the different lyophilization statuses, and storage with or without methanol. The volcano plot shows a broadly balanced distribution of up- and downregulated features between homogenization and the double-liquid extraction. However, features upregulated under double-liquid extraction display a wider dispersion in both fold change and statistical significance (Fig. 4A). Pathway annotation of significantly altered features within the Sankey diagram highlights extraction preferences for specific compound classes (Fig. 4B). Amino acids including proline (CL2), aspartic acid (CL1), tyrosine (CL2), and tryptophan (CL1) were significantly upregulated in samples processed using the DLE protocol. Additionally, a series of glycine-containing dipeptides, such as glycyl-phenylalanine (CL2) and glycyl-tyrosine (CL1), were also enriched under the DLE conditions. Based on these results, amino acids and short peptides exhibited a higher extraction efficiency and broader coverage with the DLE extraction method compared to methanol-based homogenization. This effect is likely attributable to the physicochemical properties of DMSO, which is known to induce a reduction of the cell membrane and an increase of the membrane fluidity, thereby facilitating the release of intracellular and matrix-associated polar metabolites.[35] Representative boxplots of five selected metabolites within sample-preparation factor are shown in Fig. 4C. Boxplots of a selection of annotated significant metabolites are provided in the SI. Due to the partially unbalanced design, estimated effects represent conditional comparisons within the observed data structure rather than fully orthogonal factor effects. As a result, partial confounding between workflow factors and sampling day cannot be fully excluded.

In contrast, methanol rapidly denatures proteins and promotes localized aggregation, which can entrap small polar metabolites and reduce their effective recovery. Consistent with this interpretation, heterocyclic nucleobases and nucleosides, including inosine (CL2), guanosine (CL2), and uracil

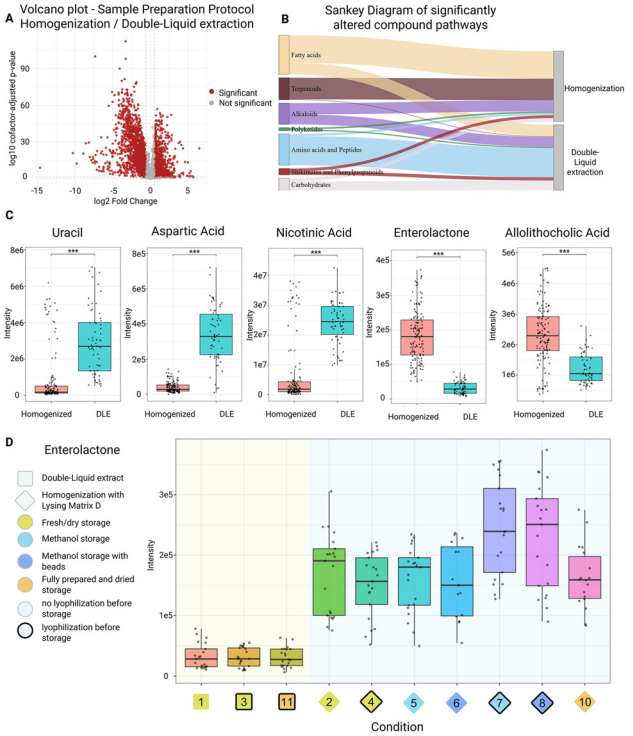

Fig. 4 Statistical overview of sample preparation protocol effect on long-term storage. (A) Volcano plot of the sample preparation protocol effect of individual metabolomic features (n = 8895, significance = 3228). Y-Axis utilizing −log10 of p-value (<0.05) obtained with linear model with cofactor adjustment, where collection day, lyophilization, and methanol storage status before storage were adjusted for. The x-axis represents the log2 fold change (>1.5 or <1/1.5) of estimated marginal means (EMM). Significantly altered features denoted with red color. (B) Sankey diagram of NPClassifier-predicted pathways of significantly altered metabolites (n = 436). Line thickness corresponds to the relative number of metabolites per pathway. (C) Boxplots of annotated significantly altered metabolites (annotation confidence level ≥ 2). Statistical significance within a factor is indicated as: *** p < 0.001, ** p < 0.01, * p < 0.05. Group colors: storage without methanol – magenta; storage with methanol – cyan. (D) Extended boxplot of enterolactone (CL = 1) with 10 experimental conditions compared. Each condition denoted with different color, as well as coded by 3 categories, with legend to the left of the plot area.

(CL2), were also significantly upregulated in samples processed *via* the DLE workflow. These compounds have a high polarity and have been associated with microbial nucleotide turnover, making their recovery particularly sensitive to solvent polarity and protein precipitation.[36] In contrast, methanol-based homogenization demonstrated a slightly improved extraction of more hydrophobic metabolites. Lipid-associated compounds such as hexadecasphingosine (CL2), sphingosine (CL2), and *N*-lauroyl glutamic acid (CL2) were upregulated in methanol-homogenized samples, consistent with the strong solubilizing capacity of methanol for amphipathic and lipid-like molecules.[37] Microbial metabolites and gut microbiota metabolized dietary compounds like enterolactone (CL1) and solanidine (CL2) were also significantly affected by beads homogenization protocols compared with the DLE protocol. This suggests that their recovery depends strongly on the mechanical disruption and extraction solvents. As an example, a more detailed examination of individual sample preparation conditions revealed that the dependence of enterolactone levels on the preparation method with lower values with the double liquid extraction. One potential reason is that the aqueous conditions may promote reduced recovery and partial lactone ring opening under hydrolytic sample preparation conditions (Fig. 4D). In contrast, the highly polar and water-soluble vitamin pantothenic acid (CL2) was significantly downregulated under methanol-extraction conditions, which further supports the assumption that methanol homogenization has limited extraction efficiency for small polar metabolites.

To specifically assess the performance of lysing matrix E, we compared Condition 9 with Condition 6, which serves as its lysing matrix D counterpart, as all other experimental factors were identical. Sampling day was included as a cofactor in the statistical model. This comparison revealed more than 700 features showing significant differences (p < 0.05, fold change ≥ 1.5). Annotation and compound-class prediction suggested that lysing matrix E preferentially enhanced extraction of carbohydrates, shikimates, and alkaloids such as nicotinic acid (CL1), adenine (CL1) and guanine (CL1). These metabolite classes are commonly associated with intracellular pools or metabolites localized within microbial cells, which is consistent with the design of Matrix E beads that include smaller spheres intended to improve microbial cell disruption and release of intracellular content. In contrast, lysing matrix D showed higher abundances of several features tentatively annotated at CL 3 as indoles or compounds from the tryptophan pathway. As lysing matrix E contains additional smaller beads for optimized homogenization of microbial cells, the upregulation of these microbial metabolites is a result of an improved release of intra-cellular bacterial content. Additional targeted validation is required to confirm whether these observations reflect systematic extraction biases or compound-specific effects. Comparative highlights of lysing matrices D and E are provided in the SI (Fig. S1).

Freeze-drying is commonly employed to stabilize fecal material, normalization, simplify storage, and improve homogeneity. However, its impact on the metabolite profiles remains insufficiently studied. Comparison of fresh and freeze-dried conditions demonstrated a partial overlap with some separation in the PCA (Fig. 3C), indicating that lyophilization introduces systematic chemical shifts. Freeze-drying may alter microbial enzymatic activity and volatile compounds differently prior to drying and after thawing than with the other sample preparation processes. Despite these differences, freeze-dried samples demonstrated relatively low within-group dispersion, suggesting that lyophilization produces a chemically more stable matrix.

Application of a cofactor-adjusted linear model identified that the majority of significantly altered features were associated with extraction conditions without lyophilization were used. The volcano plot clearly shows larger numbers of 2649 upregulated features for samples that were not lyophilized

compared to 147 downregulated features (Fig. 5A). Among the annotated metabolic pathways, metabolites within the Fatty acids, Alkaloids and Amino acids and short peptides were the ones of the most affected (Fig. 5B). The following metabolites from diverse compound classes, particularly pantothenic acid (CL2), spiculisporic acid (CL2), nicotinic acid (CL1), and xanthine (CL2) have been found to be significantly upregulated in samples that were prepared without prior lyophilization. Several studies have reported that lyophilization can increase the number of metabolites due to enhanced cell lysis or membrane disintegration, while volatile metabolites are at risk of being removed.[38,39] In contrast, our data shows that fresh fecal samples provide a broader metabolite coverage and higher extraction efficiency in comparison to lyophilized samples. Reduced performance of freeze-dried samples extracted in pure methanol may be due to insufficient rehydration or altered solvent–matrix interactions of the dried matrix. In the DLE protocol, the samples that were reconstituted with a 5% DMSO/water solution under sonication yielded a lower homogenization effect in comparison to the beads-based homogenizer due to insufficient mechanical disruption. This is potentially limiting the release of intracellular and matrix-associated metabolites. The reason for the detection of amino acid derivatives at reduced levels in the lyophilized samples exemplified by proline (CL2), valyl-valine (CL2), ophthalmic acid (CL1), and 4-guanikdinobutanoic acid (CL1/Fig. 5C). As summary, while sufficient homogenization is achieved in the bead homogenization protocol, the pure methanol solution had a reduced efficiency for highly polar compounds.

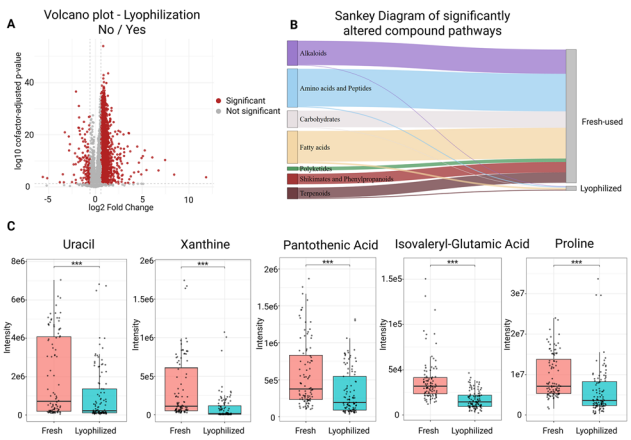

Fig. 5 Statistical overview of lyophilization effect on long-term storage. (A) Volcano plot of the lyophilization effect of individual metabolomic features (n = 8895, signif.n. = 2797). Y-Axis utilizing −log10 of p-value (<0.05) obtained with linear model with cofactor adjustment, where collection day, sample preparation protocol, and methanol storage status before storage were adjusted for. The x-axis represents the log2 fold change (>1.5 or <1/1.5) of estimated marginal means (EMM). Significantly altered features denoted with red color. (B) Sankey diagram of NPClassifier-predicted pathways of significantly altered metabolites (n = 318). Line thickness corresponds to the relative number of metabolites per pathway. (C) Boxplots of annotated significantly altered metabolites (annotation confidence level ≥ 2b). Statistical significance within a factor is indicated as: *** p < 0.001, ** p < 0.01, * p < 0.05. Group colors: storage without methanol – magenta; storage with methanol – cyan.

Next, we investigated whether performing the majority of the sample preparation workflow immediately when receiving samples and before long-term storage has a positive affected on the metabolome stability or not. The PCA demonstrated partial separation between samples prepared before storage and those prepared after thawing (Fig. 3D), while the magnitude of this effect was smaller relative to freeze-drying or methanol exposure. These findings support the idea that completing as many extraction steps as possible before long-term storage can potentially reduce variability. It needs to be decided if the observed minor effect is sufficient to compensate for the increased complexity of sample handling and collection to storage timing.

Because fecal material remains enzymatically and microbially active immediately after collection, some workflows use organic solvents such as methanol to deactivate biological processes and stabilize metabolites before storage. PCA analyses indicate that methanol exposure during long-term storage produced a small shift in the global metabolite composition with a substantial overlap between conditions (Fig. 3E).

To relatively quantify these differences, we performed a linear regression model adjusting for the sampling day, extraction protocol, and freeze-dry status. Methanol storage significantly affected 381 out of 8895 metabolomic features, with both increases and decreases observed across diverse chemical classes. NPClassifier annotation of the significantly altered features revealed that several molecular families were particularly impacted by methanol storage. While methanol exposure at a global level during long-term storage resulted in only minor compositional shifts, more pronounced differences were observed for individual features, metabolites and specific metabolite classes. Within the amino acids and peptide derivatives pathways, *N*-acetyl-phenylalanine (CL1) and nicotinic acid (CL1) were significantly reduced under methanol storage. Similarly, nucleotide-related metabolites, like xanthine (CL2) were significantly reduced in the samples stored in methanol (Fig. 6A). These shifts may reflect methanol-induced chemical extraction biases, selective solubilization of polar metabolites or quenching of enzymatic pathways that otherwise lead to production of metabolites during the storage. While these changes are limited to a global context, they are analytically relevant for studies targeting specific metabolite classes sensitive to the investigated conditions. Notably, uracil (CL2) exhibited a distinct and informative behaviour. Although it appeared significantly altered across multiple experimental factors, the drivers of its elevated levels in condition 2 (homogenized after storage from wet sample) were not immediately evident. Closer analysis revealed that uracil was consistently upregulated under the DLE protocol, whereas it was either absent or detected only at trace levels in methanol-stored samples. One-way ANOVA followed by Tukey's HSD *post-hoc* test revealed no significant differences among methanol-stored conditions irrespective of when bead-beating homogenization was applied (Fig. 6B). Lyophilization combined with subsequent homogen-

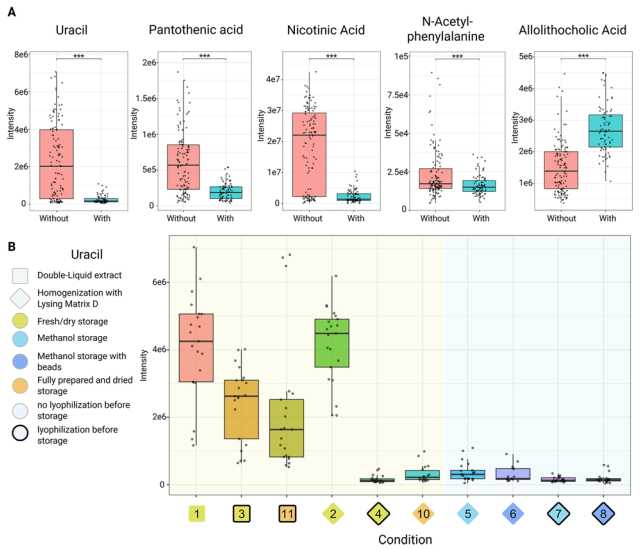

Fig. 6 Statistical overview of long-term storage with and without methanol. (A) Boxplots of annotated significantly altered metabolites (annotation confidence level ≥ 2b). Statistical significance within a factor is indicated as: *** $p < 0.001$, ** $p < 0.01$, * $p < 0.05$. Group colors: storage without methanol – magenta; storage with methanol – cyan. (D) Extended boxplot of uracil with all 10 experimental conditions compared. Each condition denoted with different color, as well as coded by 3 categories, with legend to the left of the plot area.

ization under methanol-based extraction resulted in a pronounced reduction in uracil abundance. Together, these observations indicate that uracil levels are primarily influenced by extraction chemistry with no significant dependence on whether extraction was performed before or after long-term storage, if methanol extraction is preferred, storage must be performed with not lyophilized or solvated sample (Fig. 6B).

The consistent suppression of these metabolites suggests that long-term methanol storage may promote degradation or reduce the extraction efficiency. This potential effect needs to be considered for the interpretation of studies targeting nucleosides, vitamins, or purine metabolism.[40] In contrast, the higher levels observed in samples stored without methanol may reflect DNA degradation by microbial activity, suggesting a greater level of microbial suppression by methanol storage. Targeted comparisons of individual sample preparation factors, compound classes, and representative metabolites provide particular insights into the most significantly altered differences. Several metabolites can be identified to be significantly altered in a global perspective, however, these do not retain significance for individual factor comparison after cofactor adjustment. This suggests that their variance was distributed across multiple experimental variables rather than driven by a single preparation or storage factor. For example, methylthioadenosine sulfoxide (CL1) and 6-hydroxycoumaran (CL1) exhibited significant differences across all grouping factors, indicating that these compounds are broadly sensitive to sample handling and storage conditions. Contrary, 4-vinylphenol (CL1) was not observed with significant variations across any the tested conditions, suggesting a high degree of robustness to differences in sample preparation and storage.

Conclusion

In this study, we conducted a comprehensive metabolomics evaluation of multiple combinations of sample preparation protocols and long-term storage conditions for human fecal samples. We compared two preparation strategies and assessed the impact of key workflow steps, including freeze-drying and methanol exposure. This study provides a systematic evaluation of combined preparation and storage workflows, including pre-storage freeze-drying and long-term methanol exposure, within a unified analytical framework.

Our results reveal a metabolomic profile shift associated with long-term methanol storage, particularly affecting purine and pyrimidine-related metabolites when compared with freezing of fresh material. At the global level, selectivity and sensitivity analyses revealed consistent, yet relatively modest, differences between sample preparation and storage conditions, particularly when contrasted with the pronounced day-to-day variability observed across sampling days. This temporal variability likely reflects biological and pre-analytical factors such as diet and sampling time, which highlights the inherent complexity of fecal metabolomics. As this study is based on repeated sampling from a single individual, these observations reflect workflow-dependent effects within a controlled biochemical background without capturing inter-individual variability.

Despite this dominant day-to-day variability, compound-class-specific analyses revealed reproducible preferences for particular extraction and storage strategies. Protocols incorporating beads-based homogenization of non-lyophilized samples generally provided broader metabolite coverage and higher signal intensities, supporting their suitability for untargeted applications. When freeze-drying is required, reintroduction of water prior to extraction appears important for preserving extraction efficiency, particularly for polar metabolites. While exhibiting intermediate global performance, the DLE protocol demonstrated comparatively consistent performance across replicates and sampling days, suggesting potential utility in workflows where methodological flexibility is required.

Several practical considerations can be outlined based on the data in this study. For broad untargeted metabolite coverage and higher signal intensities, protocols incorporating bead-based homogenization of non-lyophilized samples are generally preferred. For polar metabolites, extraction conditions that preserve or reintroduce water should be prioritized, while extraction in pure methanol after freeze-drying may reduce coverage. For workflows requiring long-term storage without immediate processing, methanol-based storage introduces only modest global variation but may selectively affect specific metabolite classes. For studies prioritizing consistency across preparation and storage conditions, the

DLE protocol provides stable performance with moderate global coverage.

In summary, our findings emphasize that the choice of sample preparation and storage strategy should be guided by the analytical objective of global analysis and the metabolite classes of interest in targeted applications. Maintaining the same sample handling procedure for all samples remains the most essential factor to minimize technical and preanalytical variability. Overall, our results provide a comparative analytical overview of how sample preparation and storage workflows influence the fecal metabolome. Our data provides new information for method selection within controlled experimental designs. Translation of these findings to broader clinical or population-level studies requires further validation across clinical cohorts.

Author contributions

VD: methodology, investigation, formal analysis, data curation, validation, visualization, writing – original draft. DG: supervision, project administration, funding acquisition, methodology, data curation, conceptualization, writing – original draft.

Conflicts of interest

There are no conflicts to declare.

Data availability

The main findings are presented in Fig. 1–6 and Fig. S1–S5. The Supplementary Table S1 contains the metabolomics output data and statistics. The UHPLC-MS RAW-data and data output files can be obtained from the corresponding author upon reasonable request.

Supplementary information (SI) is available. See DOI: https://doi.org/10.1039/d6an00237d.

Acknowledgements

We highly appreciate the support from the Swedish Research Council (VR 2020-04707) and the Swedish Cancer Society (22 2449 Pj, 25 4898 Pj) to D. G.

References

1 N. Karu, L. Deng, M. Slae, A. C. Guo, T. Sajed, H. Huynh, E. Wine and D. S. Wishart, *Anal. Chim. Acta*, 2018, **1030**, 1–24.
2 J. Zierer, M. A. Jackson, G. Kastenmüller, M. Mangino, T. Long, A. Telenti, R. P. Mohney, K. S. Small, J. T. Bell, C. J. Steves, A. M. Valdes, T. D. Spector and C. Menni, *Nat. Genet.*, 2018, **50**, 790–795.
3 K. S. Smirnov, T. V. Maier, A. Walker, S. S. Heinzmann, S. Forcisi, I. Martinez, J. Walter and P. Schmitt-Kopplin, *Int. J. Med. Microbiol.*, 2016, **306**, 266–279.
4 A. Tronel, M. Roger-Margueritat, C. Plazy, V. Cunin, I. Mohanty, P. C. Dorrestein, T. Soranzo and A. Le Gouellec, *Metabolomics*, 2025, **21**, 84.
5 Y. K. Yeoh, Z. Chen, M. Hui, M. C. S. Wong, W. C. S. Ho, M. L. Chin, S. C. Ng, F. K. L. Chan and P. K. S. Chan, *PeerJ*, 2019, **7**, e6172.
6 A. Schultze, M. K. Akmatov, M. Andrzejak, N. Karras, Y. Kemmling, A. Maulhardt, S. Wieghold, W. Ahrens, K. Günther, H. Schlenz, G. Krause and F. Pessler, *Bundesgesundheitsblatt Gesundheitsforschung Gesundheitsschutz*, 2014, **57**, 1264–1269.
7 H. Isokääntä, L. Pinto Da Silva, N. Karu, T. Kallonen, A.-K. Aatsinki, T. Hankemeier, L. Schimmel, E. Diaz, T. Hyötyläinen, P. C. Dorrestein, R. Knight, M. Orešič, R. Kaddurah-Daouk, A. M. Dickens and S. Lamichhane, *Anal. Chem.*, 2024, **96**, 8893–8904.
8 K. Kruger, Y. Myeonghyun, N. Van Der Wielen, D. E. Kok, G. J. Hooiveld, S. Keshtkar, M. Diepeveen-De Bruin, M. G. J. Balvers, M. Grootte-Bromhaar, K. Mudde, N. T. H. N. Ly, Y. Vermeiren, L. C. P. G. M. De Groot, R. C. H. De Vos, G. B. Gonzales, W. T. Steegenga and M. P. H. Van Trijp, *Sci. Rep.*, 2024, **14**, 115829.
9 M. De Spiegeleer, M. De Graeve, S. Huysman, A. Vanderbeke, L. Van Meulebroek and L. Vanhaecke, *Anal. Chim. Acta*, 2020, **1108**, 79–88.
10 V. O'Sullivan, F. Madrid-Gambin, T. Alegra, H. Gibbons and L. Brennan, *ACS Omega*, 2018, **3**, 16585–16590.
11 O. Deda, H. G. Gika, I. D. Wilson and G. A. Theodoridis, *J. Pharm. Biomed. Anal.*, 2015, **113**, 137–150.
12 J. Gratton, J. Phetcharaburanin, B. H. Mullish, H. R. T. Williams, M. Thursz, J. K. Nicholson, E. Holmes, J. R. Marchesi and J. V. Li, *Anal. Chem.*, 2016, **88**, 4661–4668.
13 J. M. Choo, L. E. Leong and G. B. Rogers, *Sci. Rep.*, 2015, **5**, 16350.
14 R. Tautenhahn, G. J. Patti, D. Rinehart and G. Siuzdak, *Anal. Chem.*, 2012, **84**, 5035–5039.
15 E. M. Forsberg, T. Huan, D. Rinehart, H. P. Benton, B. Warth, B. Hilmers and G. Siuzdak, *Nat. Protoc.*, 2018, **13**, 633–651.
16 S. Fan, T. Kind, T. Cajka, S. L. Hazen, W. H. W. Tang, R. Kaddurah-Daouk, M. R. Irvin, D. K. Arnett, D. K. Barupal and O. Fiehn, *Anal. Chem.*, 2019, **91**, 3590–3596.
17 S. R. Searle, F. M. Speed and G. A. Milliken, *Am. Stat.*, 1980, **34**, 216–221.
18 D. S. Wishart, A. Guo, E. Oler, F. Wang, A. Anjum, H. Peters, R. Dizon, Z. Sayeeda, S. Tian, B. L. Lee, M. Berjanskii, R. Mah, M. Yamamoto, J. Jovel, C. Torres-Calzada, M. Hiebert-Giesbrecht, V. W. Lui, D. Varshavi, D. Varshavi, D. Allen, D. Arndt, N. Khetarpal, A. Sivakumaran, K. Harford, S. Sanford, K. Yee, X. Cao, Z. Budinski, J. Liigand, L. Zhang, J. Zheng, R. Mandal,

N. Karu, M. Dambrova, H. B. Schiöth, R. Greiner and V. Gautam, *Nucleic Acids Res.*, 2022, **50**, D622–D631.
19 K. Dührkop, H. Shen, M. Meusel, J. Rousu and S. Böcker, *Proc. Natl. Acad. Sci. U. S. A.*, 2015, **112**, 12580–12585.
20 M. A. Hoffmann, L.-F. Nothias, M. Ludwig, M. Fleischauer, E. C. Gentry, M. Witting, P. C. Dorrestein, K. Dührkop and S. Böcker, *Nat. Biotechnol.*, 2022, **40**, 411–421.
21 J. Rainer, A. Vicini, L. Salzer, J. Stanstrup, J. M. Badia, S. Neumann, M. A. Stravs, V. Verri Hernandes, L. Gatto, S. Gibb and M. Witting, *Metabolites*, 2022, **12**, 173.
22 K. Dührkop, L. F. Nothias, M. Fleischauer, R. Reher, M. Ludwig, M. A. Hoffmann, D. Petras, W. H. Gerwick, J. Rousu, P. C. Dorrestein and S. Böcker, *Nat. Biotechnol.*, 2021, **39**, 462–471.
23 H. Horai, M. Arita, S. Kanaya, Y. Nihei, T. Ikeda, K. Suwa, Y. Ojima, K. Tanaka, S. Tanaka, K. Aoshima, Y. Oda, Y. Kakazu, M. Kusano, T. Tohge, F. Matsuda, Y. Sawada, M. Y. Hirai, H. Nakanishi, K. Ikeda, N. Akimoto, T. Maoka, H. Takahashi, T. Ara, N. Sakurai, H. Suzuki, D. Shibata, S. Neumann, T. Iida, K. Tanaka, K. Funatsu, F. Matsuura, T. Soga, R. Taguchi, K. Saito and T. Nishioka, *J. Mass Spectrom.*, 2010, **45**, 703–714.
24 E. L. Schymanski, J. Jeon, R. Gulde, K. Fenner, M. Ruff, H. P. Singer and J. Hollender, *Environ. Sci. Technol.*, 2014, **48**, 2097–2098.
25 W. Lin, L. P. Conway, A. Block, G. Sommi, M. Vujasinovic, J.-M. Löhr and D. Globisch, *Analyst*, 2020, **145**, 3822–3831.
26 A. Kaur, W. Lin, V. Dovhalyuk, L. Driutti, M. L. Di Martino, M. Vujasinovic, J.-M. Löhr, M. E. Sellin and D. Globisch, *Chem. Sci.*, 2023, **14**, 5291–5301.
27 V. Dovhalyuk, F. Yang, S. Nikolic, M. Vujasinovic, J. M. Löhr and D. Globisch, *United European Gastroenterol. J.*, 2025, **13**, 1560–1570.
28 I. Tsiara, M. S. P. Correia, F. Yang, W. Zeng, P. Seeburger, B. Hervás Povo, I. Lundgaard, M. Menéndez-González, M. Vujasinovic, J.-M. Löhr and D. Globisch, *Anal. Bioanal. Chem.*, 2025, DOI: 10.1007/s00216-025-06082-w.
29 M. R. Gemmell, T. Jayawardana, S. Koentgen, E. Brooks, N. Kennedy, S. Berry, C. Lees and G. L. Hold, *Sci. Rep.*, 2024, **14**, 16816.
30 K. Tarazona Carrillo, S. L. Nam, A. P. De La Mata, O. M. De Bruin, E. Doukhanine and J. Harynuk, *Metabolomics*, 2023, **19**, 74.
31 P. Yan, M. Luo, F. Liu and J. Li, *Chin. Med. J.*, 2022, **135**, 1102–1104.
32 M. Haid, C. Muschet, S. Wahl, W. Rmisch-Margl, C. Prehn, G. Mller and J. Adamski, *J. Proteome Res.*, 2018, **17**, 203–211.
33 E. Loftfield, E. Vogtmann, J. N. Sampson, S. C. Moore, H. Nelson, R. Knight, N. Chia and R. Sinha, *Cancer Epidemiol., Biomarkers Prev.*, 2016, **25**, 1483–1490.
34 N. Procházková, M. F. Laursen, G. La Barbera, E. Tsekitsidi, M. S. Jørgensen, M. A. Rasmussen, J. Raes, T. R. Licht, L. O. Dragsted and H. M. Roager, *Nat. Microbiol.*, 2024, **9**, 3210–3225.
35 A. A. Gurtovenko and J. Anwar, *J. Phys. Chem. B*, 2007, **111**, 10453–10460.
36 X. Qin and X. Wang, *J. Pharm. Biomed. Anal.*, 2018, **158**, 280–287.
37 M. Höring, S. Krautbauer, L. Hiltl, V. Babl, A. Sigruener, R. Burkhardt and G. Liebisch, *Metabolites*, 2021, **11**, 365.
38 S. L. Nam, K. Tarazona Carrillo, A. P. De La Mata, O. M. De Bruin, E. Doukhanine and J. Harynuk, *Metabolomics*, 2022, **18**, 25.
39 J. Ueyama, M. Oda, M. Hirayama, K. Sugitate, N. Sakui, R. Hamada, M. Ito, I. Saito and K. Ohno, *Anal. Biochem.*, 2020, **589**, 113508.
40 K. Kasahara, R. L. Kerby, Q. Zhang, M. Pradhan, M. Mehrabian, A. J. Lusis, G. Bergström, F. Bäckhed and F. E. Rey, *Cell Host Microbe*, 2023, **31**, 1038–1053.